BMC Cancer

RESEARCH Open Access

Curcumin suppresses colorectal tumorigenesis through restoring the gut microbiota and metabolites

Wenxin Deng[1,2†], Xiaojian Xiong[1†], Mingyang Lu[3], Shibo Huang[4], Yunfei Luo[5], Yujie Wang[1] and Ying Ying[1,6*]

Abstract

Background Curcumin has been reported to have activity for prevention and therapy of CRC, yet its underlying mechanisms remain largely unknown. Recently, emerging evidence suggests that the gut microbiota and its metabolites contribute to the causation and progression of Colorectal cancer (CRC). In this study, we aimed to investigate if curcumin affects the tumorigenesis of CRC by modulating gut microbiota and its metabolites.

Methods Forty male C57BL/6JGpt mice were randomly divided into four groups: negative control (NC), curcumin control, CRC model, and curcumin treatment (CRC-Cur) groups. CRC mouse model was induced by using azoxymethane (AOM) and dextran sodium sulfate (DSS), and the mice in CRC model and curcumin treatment groups received oral PBS or curcumin (150 mg/kg/day), respectively. Additionally, fecal samples were collected. 16 S rRNA sequencing and Liquid Chromatography Mass Spectrometry (LC-MS)-based untargeted metabolomics were used to observe the changes of intestinal flora and intestinal metabolites.

Results Curcumin treatment restored colon length and structural morphology, and significantly inhibited tumor formation in AOM/DSS-induced CRC model mice. The 16S rRNA sequencing analysis indicated that the diversity and richness of core and total species of intestinal microflora in the CRC group were significantly lower than those in the NC group, which were substantially restored in the curcumin treatment group. Curcumin reduced harmful bacteria, including *Ileibacterium*, *Monoglobus* and *Desulfovibrio*, which were elevated in CRC model mice. Moreover, curcumin increased the abundance of *Clostridia_UCG-014*, *Bifidobacterium* and *Lactobacillus*, which were decreased in CRC model mice. In addition, 13 different metabolites were identified. Compared to the NC group, ethosuximide, xanthosine, and 17-beta-estradiol 3-sulfate-17-(beta-D-glucuronide) were elevated in the CRC model group, whereas curcumin treatment significantly reduced their levels. Conversely, glutamylleucine, gamma-Glutamylleucine, liquiritin, ubenimex, 5′-deoxy-5′-fluorouridine, 7,8-Dihydropteroic acid, neobyakangelicol, libenzapril, xenognosin A, and 7,4′-dihydroxy-8-methylflavan were decreased in the CRC group but notably upregulated by curcumin. Kyoto Encyclopedia of Genes and Genome (KEGG) pathway analysis revealed enrichment in seven pathways, including folate biosynthesis ($P < 0.05$).

†Wenxin Deng and Xiaojian Xiong contributed equally to this work and shared the first authorship.

*Correspondence:
Ying Ying
yingying@ncu.edu.cn

Full list of author information is available at the end of the article

Conclusions The gut microecological balance was disrupted in AOM/DSS-induced CRC mice, accompanied by metabolite dysbiosis. Curcumin restored the equilibrium of the microbiota and regulated metabolites, highly indicating that curcumin may alleviate the development of AOM/DSS induced colorectal cancer in mice by regulating intestinal flora homeostasis and intestinal metabolites.

Keywords Curcumin, Colorectal cancer, Gut microbiota, Metabolites

Introduction

Colorectal cancer (CRC) is the third most common malignant tumor globally, posing a severe threat to human health, with a steadily increasing incidence [1]. Current CRC treatments primarily involve a combination of surgery, chemotherapy, radiotherapy, and immunomodulatory therapy [2, 3]. Traditional therapies are expensive, prone to chemotherapy resistance, and associated with serious side effects, leading to poor patient prognosis and increased mortality [4]. Hence, there is an urgent need to explore safe and effective therapeutic drugs or novel treatment approaches to inhibit or even reverse disease progression.

Although the exact pathogenic mechanisms of CRC remain unclear, research has demonstrated a clear association between disruption of the host-microbiota and CRC, as trillions of gut microbes and their metabolites interact directly with the intestinal canal [5]. Early studies have shown that fecal samples from CRC patients induced intestinal carcinogenesis in mice [6]. Moreover, research has demonstrated that certain bacteria, such as *Fusobacterium nucleatum* and *Bacteroides fragilis*, can promote CRC progression [7]. Further studies indicate that the effects of the CRC-associated gut microbiota are closely linked to its metabolite. For instance, formate has been shown to promote CRC progression, while most short-chain fatty acids are believed to inhibit intestinal tumors [8, 9]. Hence, adjusting the gut microbiota population or its metabolite could be a viable approach for CRC treatment.

The preventive and therapeutic effects of traditional Chinese medicine on CRC have garnered increased amounts of attention in recent years. Curcumin is a polyphenolic compound extracted from the rhizomes of turmeric plants [10]. Numerous studies have shown that curcumin has beneficial effects, such as antioxidant, anti-inflammatory, antitumor, antimicrobial, lipid regulatory, and analgesic effects [11–13]. While the anticancer properties of curcumin have been extensively investigated, the precise mechanisms to suppress CRC development remain unclear. Recent studies have demonstrated that curcumin inhibits the proliferation and metastasis of CRC by suppressing inflammatory responses, inducing cell cycle arrest and promoting apoptosis [14, 15]. It also exerts antitumor effects by regulating non-coding RNAs, including lncRNAs, miRNAs, and circRNAs, which impact the epigenetic control of oncogenes and tumor suppressor genes [16, 17]. Further research has confirmed that curcumin modulates drug resistance in CRC cells [18]. Based on this, preclinical studies have shown that curcumin may serve as an adjuvant to enhance the efficacy of chemotherapy [19].

Notably, research suggests curcumin may regulate gut microbiota, including its abundance, diversity, and composition to improve microbiota composition, thus influencing the gut microbiome [20]. This regulatory effect has been found to alleviate various conditions such as colitis and hepatic steatosis [21, 22]. Additionally, changes in metabolic products induced by curcumin may also suggest beneficial effects on diseases like obesity [23, 24]. Therefore, we hypothesize that curcumin may inhibit CRC by modulating the gut microbiota population and its metabolic products.

In this study, we established an azoxymethane plus dextran sulfate sodium (AOM/DSS)-induced CRC model to investigate whether curcumin influences CRC tumorigenesis and progression through its specific regulatory effects on gut microbiota and metabolites. Our findings showed that curcumin mitigated the pathological progression of CRC and reduced tumor incidence. Further analysis revealed that curcumin treatment improved the gut microbiota population in mice and favorably modulated 13 bacterial metabolites levels, which may be a key mechanism for its preventive and therapeutic effects against CRC.

Materials and methods

Animal experiments

All animal experiments were conducted in compliance with the ethical standards set by the Experimental Animal Ethics Committee of Nanchang University, following the guidelines for standard experimental animals. C57BL/6JGpt mice (male, weighing 18–23 g, aged 6–8 weeks) were obtained from Jiangsu JieCui YaoKang Biotechnology Co., Ltd. All the animals were housed in a secondary barrier facility with controlled environmental conditions, maintaining a temperature of 24–25 °C and relative humidity between 45% and 50%. The mice were provided SPF-grade feed, sterilized water and bedding.

For the CRC and curcumin-CRC groups, mice were intraperitoneally injected with 10 mg/kg of AOM. From days 5–10, 24–29, and 43–48, the mice were given drinking water containing 2% DSS, with regular water provided on the other days. Starting on day 5, mice in the

curcumin-CRC group received daily oral gavage of curcumin at 150 mg/kg, while the CRC group received the same volume of PBS. Similarly, mice in the NC group and curcumin group were intraperitoneally injected with sterile saline and had free access to regular water. Curcumin or PBS was administered intragastrically to these groups as well. Routine feeding and close observation of mouse activity were maintained throughout the modeling period. After euthanizing the mice using carbon dioxide asphyxia, we performed careful dissections to collect the colorectal tissues and their contents.

Hematoxylin-eosin (HE) staining

The fixed colorectal tissues were removed from the 4% paraformaldehyde solution and placed in tissue embedding cassettes, followed by processing in an automatic tissue dehydrator (Excelsior™ AS; Thermo Scientific, USA) with a specified dehydration program. Subsequently, the colorectal tissues were embedded in paraffin blocks (HistoStar; Thermo Scientific, USA) and cut into 5 μm thick tissue sections. The tissue sections were affixed to adhesive slides. Paraffin-embedded sections were dewaxed with xylene and rehydrated with graded concentrations of alcohol. The cell nuclei were stained with hematoxylin for 10 min, followed by rinsing with water. Differentiation was achieved with 1% hydrochloric acid alcohol for 1 s, followed by counterstaining with 0.05% lithium carbonate for 3 s and rinsing for 10 min. Subsequent eosin staining solution was applied for 5 min to stain the cytoplasm. After dehydration and drying, the slides were fixed with neutral gum, and images were collected and stored using a digital slide scanner (VS200; Olympus, Japan).

Gut microbiota 16 S rRNA sequencing analysis and data processing

The collected fecal samples were sent to Shanghai Meiji Biology Company for Illumina high-throughput sequencing of bacterial 16 S rRNA fragments. Sequencing results, based on overlap relationships, were assembled into single sequences for each paired-end (PE) fragment, followed by quality control and filtering. The filtered candidate sequences were aligned with a reference database to remove chimeric sequences, resulting in the optimal sequences. Building on the optimized sequences, operational taxonomic unit (OTU) clustering analysis and taxonomic annotation were performed, with in-depth analysis of diversity indices, taxa composition, and taxa differences. A comprehensive series of statistical and visual assessments were conducted to explore the community composition and phylogenetic evolution information of the microbial diversity present in the samples.

Metabolomic analysis via liquid chromatography mass spectrometry (LC-MS)

The collected fecal samples (each ≥200 mg) were sent to Shanghai Meiji Biology Company for untargeted metabolomic analysis. This involved the simultaneous detection and analysis of all small-molecule metabolites in the samples without specific targeting. Through intergroup comparisons, differential metabolic profiles were explored. The samples were first subjected to component separation using liquid chromatography, after which individual components entered the ion source of the high vacuum mass spectrometer for ionization. Based on the mass-to-charge ratio (m/z), the components were separated, generating mass spectra. The obtained spectral data were then analyzed to derive qualitative and quantitative results for the samples.

Statistical analysis

The experimental data were subjected to statistical analysis using SPSS, and GraphPad Prism 8 software was used for data processing and visualization. All the data are presented as the means ± standard error of the mean (SEM). For comparisons between two groups at the same time point, a t test or one-way ANOVA was performed. Two-way ANOVA was applied for intergroup comparisons at different points. A significance level of $P<0.05$ was considered to indicate statistical significance.

Results

Curcumin suppresses CRC in AOM/DSS-induced CRC mice

In order to investigate the effects of curcumin on the carcinogenesis of CRC, CRC model was induced by using AOM/DSS, and the mice received an oral gavage of PBS or curcumin treatment. The dosage of curcumin was 150 mg/kg daily, and the mice were harvested on day 87 (Fig. 1A). As shown in Fig. 1B, we found that the body weight of mice in the NC group and the curcumin group showed a gradual increase, and the overall growth trend remained consistent, indicating that administering curcumin alone did not affect the weight of the mice. In contrast, the body weight of the CRC model group decreased significantly after the first DSS administration ($P<0.05$). However, gavage with curcumin did not alleviate the overall reduction in mouse body weight during the replication of the AOM/DSS-induced CRC model ($P>0.05$; Fig. 1B). Compared with the NC group, the CRC model group exhibited a marked reduction in colon length ($P<0.0001$, Fig. 1C) and an obvious increase in tumor count ($P<0.0001$, Fig. 1D), while curcumin treatment increased the length of the colon in model mice (with no significant difference) and markedly reduced the number of tumors ($P<0.05$, Fig. 1D). Histological examination of colon slices (Fig. 1E) confirmed that mice in the NC group and the curcumin group displayed an

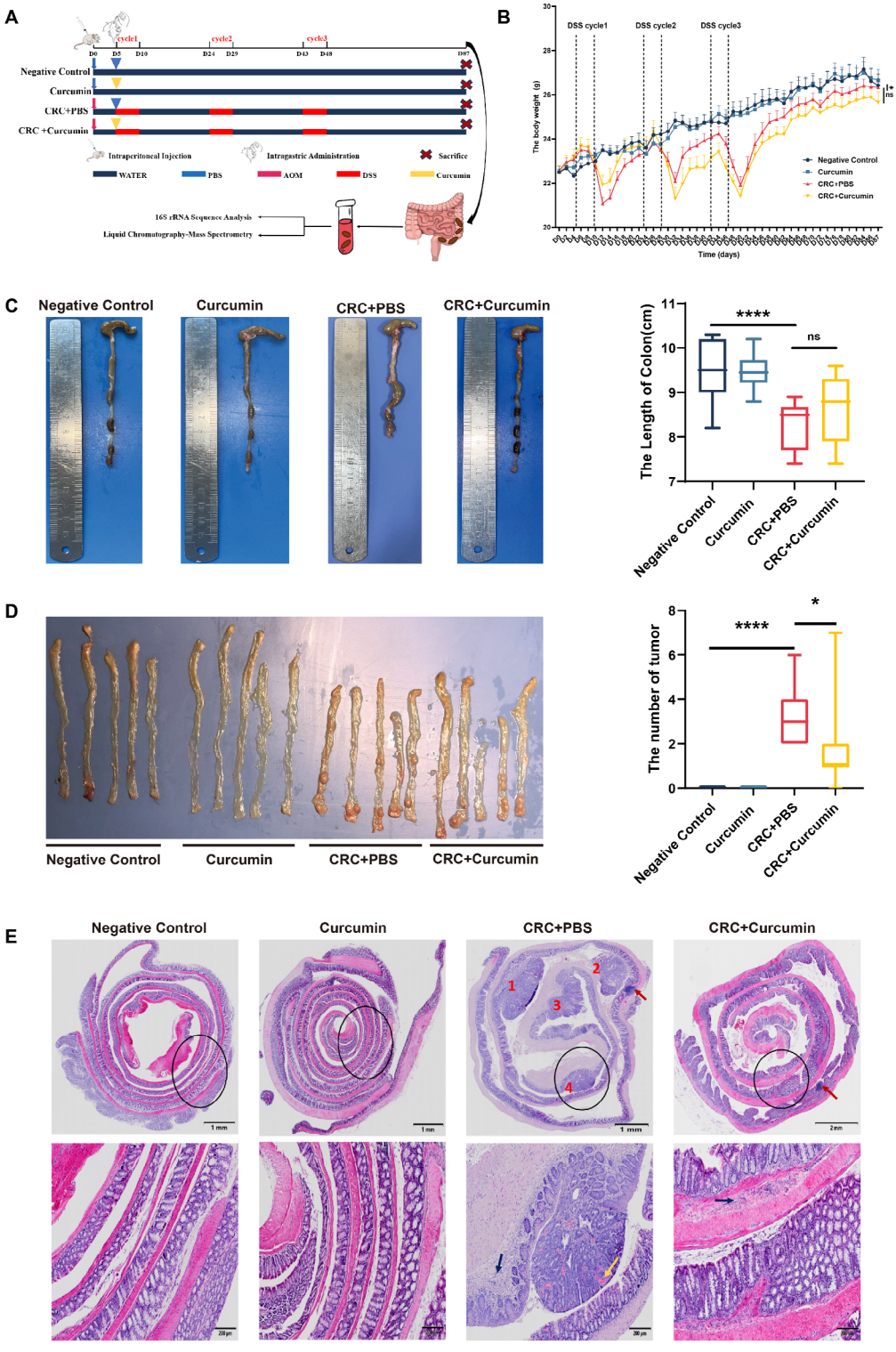

Fig. 1 Curcumin inhibits the tumorigenesis of CRC in AOM/DSS mouse model. (**A**) Experimental design for the AOM/DSS-induced CRC mouse model. (**B**) Body weights of the mice throughout the modeling period. (**C**) Representative images and length of the colorectum at sacrifice. (**D**) Colorectal anatomy diagram and tumor number. (**E**) Representative images of H&E staining of the colorectum in the NC group, curcumin-only group, and CRC model group with or without curcumin treatment. Tumor order and location are indicated by numbers 1, 2, 3, and 4. Red arrows denote lymphocyte infiltration, yellow arrows indicate red blood cells, and blue arrows represent infiltration by polymorphic nuclear cells. Scale bars: 1 mm (top) and 200 μm (bottom). The data are presented as the means ± SEMs. $^{*}p < 0.05$, $^{****}p < 0.01$. $n = 10$

intact structure. Nevertheless, the colons of model mice exhibited intraepithelial dysplasia, deformation of crypt structures, and a large accumulation of lymphocytes. The presence of polyps, which contain a considerable number of red blood cells within their interior, was observed. Gavage with curcumin restored the normal morphological structure of the colon in model mice, with no polyp formation. These findings strongly indicate that curcumin effectively inhibits CRC development induced by AOM/DSS in mice.

Curcumin modulates gut microbiome diversity in AOM/DSS-induced CRC mice

To explore the impact of curcumin on the gut microbiota of mice with CRC, we randomly selected fecal samples from five mice in each group and analyzed their intestinal microbiota using 16 S rRNA gene sequencing. We initially observed changes in the core and overall taxa abundance in each group. Core analysis (Fig. 2A) revealed that the curcumin group and CRC model group had the highest and lowest numbers of shared taxa, respectively. Compared to the CRC group, the shared taxa account of the curcumin-treated CRC group was brought to a level similar to the NC group. A similar trend was also observed in the pan analysis of total taxa (Fig. 2B). Additionally, we compared the richness and α-diversity of each microbial community by using several indices, including ace, chao, and shannon indices. As shown in Fig. 2C-E, the curcumin-CRC group exhibited a notable increase in both the ace and chao richness indices ($P<0.05$ and $P<0.01$, respectively) compared to the CRC model group. Additionally, there was an obvious increase in the shannon diversity index ($P<0.05$). These results suggest that in the gut microbiota of AOM/DSS-induced mice with CRC, there is a decrease in core taxa, total taxa, α-diversity, and richness. However, curcumin restored the intestinal microbiota in these mice.

We also investigated the differences in β-diversity. Hierarchical clustering analysis (HCA) (Fig. 2F) revealed a similarity in the composition of the gut microbiota at the phylum level between the NC and curcumin groups. While the similarity was also observed between the CRC group and the curcumin-CRC group, there are indeed slight differences in their microbiota compositions. Principal coordinate analysis (PCoA) demonstrated that, except for the variation within the NC group, the microbial community structures of the curcumin group, CRC model group, and curcumin-CRC group did not display clear differences ($P=0.037<0.05$, Fig. 2G). Furthermore, similarity analysis (ANOSIM/Adonis) (Fig. 2H) confirmed that the median line between groups was lower than that of the NC group but higher than the other three groups, indicating greater differences between groups than within each group.

Curcumin alters the gut microbiota composition and abundance in mice

LEfSe analysis identified significant differences in taxa among the four groups. As shown in Fig. 3A-B, the characteristic taxa for the NC group included *Bacteroidota* (P)-*Odoribator* (G), *Firmicutes* (P)-*Fecalibaculum* (G), and *Firmicutes* (P)-*Blautia* (G). The curcumin group included *Patescibacteria* (P)-*Candidatus* (G), *Actinobacteriota* (P)-*Bifidobacterium* (G), and *Firmicutes* (P)- *Clostridia-UCG-014* (G). The CRC group exhibited *Desulfobacterota* (P)-*Desulfovibrio* (G) and *Firmicutes* (P)-*Ileibacterium* (G) as characteristic taxa. The curcumin-treated CRC group displayed *Firmicutes* (P)-*Monoglobus* (G), *Firmicutes* (P)-*Turicibacter* (G), *Firmicutes* (P)-*Dubosiella* (G), *Firmicutes* (P)-*Roboutsia* (G), and *Firmicutes* (P)-*Clostridium* (G) as characteristic taxa. Compared to the NC group, the abundance of harmful bacteria *Desulfovibrio* and *Ileibacterium* increased and became dominant in the CRC model group. However, the curcumin-CRC group exhibited a higher abundance of normal (*Clostridium*) or beneficial (*Turicibacter*, *Dubosiella*, *Roboutsia*) bacteria within Firmicutes compared to the CRC model group. These results indicate that AOM/DSS-induced CRC in mice leads to gut microbiota dysbiosis, and curcumin may restore and enhance the dominance of beneficial bacteria in the gut.

We further assessed the detailed composition and relative abundance of the gut microbiota. At the phylum level, the primary microbial community composition classifications included *Firmicutes*, *Actinobacteriota*, *Bacteroidota*, *Verrucomicrobiota*, and *Desulfobacterota* (Fig. 3C). Curcumin has already shown an impact on the gut microbiota at the phylum level. Compared to the NC group, the CRC model group exhibited a slight reduction in *Actinobacteriota*, while levels of *Desulfobacterota*, *Cyanobacteria*, and *Deferribacterota* were elevated, though these changes were not statistically significant (Fig. 3D). In contrast, curcumin treatment increased *Actinobacteriota* levels and decreased *Desulfobacterota*, *Cyanobacteria* and *Deferribacterota* levels in both NC and CRC mice (Fig. 3D). These findings suggest that curcumin positively modulates most of the gut microbiota.

Figure 3E illustrates the differences in the composition of microbial communities at the genus level among the groups of mice. The relative abundance levels suggest that curcumin broadly affects the intestinal flora (supporting Fig. 1). To be specific, in comparison to the NC group, the CRC model group exhibited an increased abundance of *Ileibacterium*, but this abundance was remarkably reduced in both the curcumin group and the curcumin-treated CRC group ($p<0.05$, Fig. 3F). A similar trend was observed in the abundances of *Monoglobus* ($p<0.10$ and $p<0.11$, Fig. 3G) and *Desulfovibrio* ($p<0.05$ and $p<0.09$, Fig. 3H). Additionally, compared

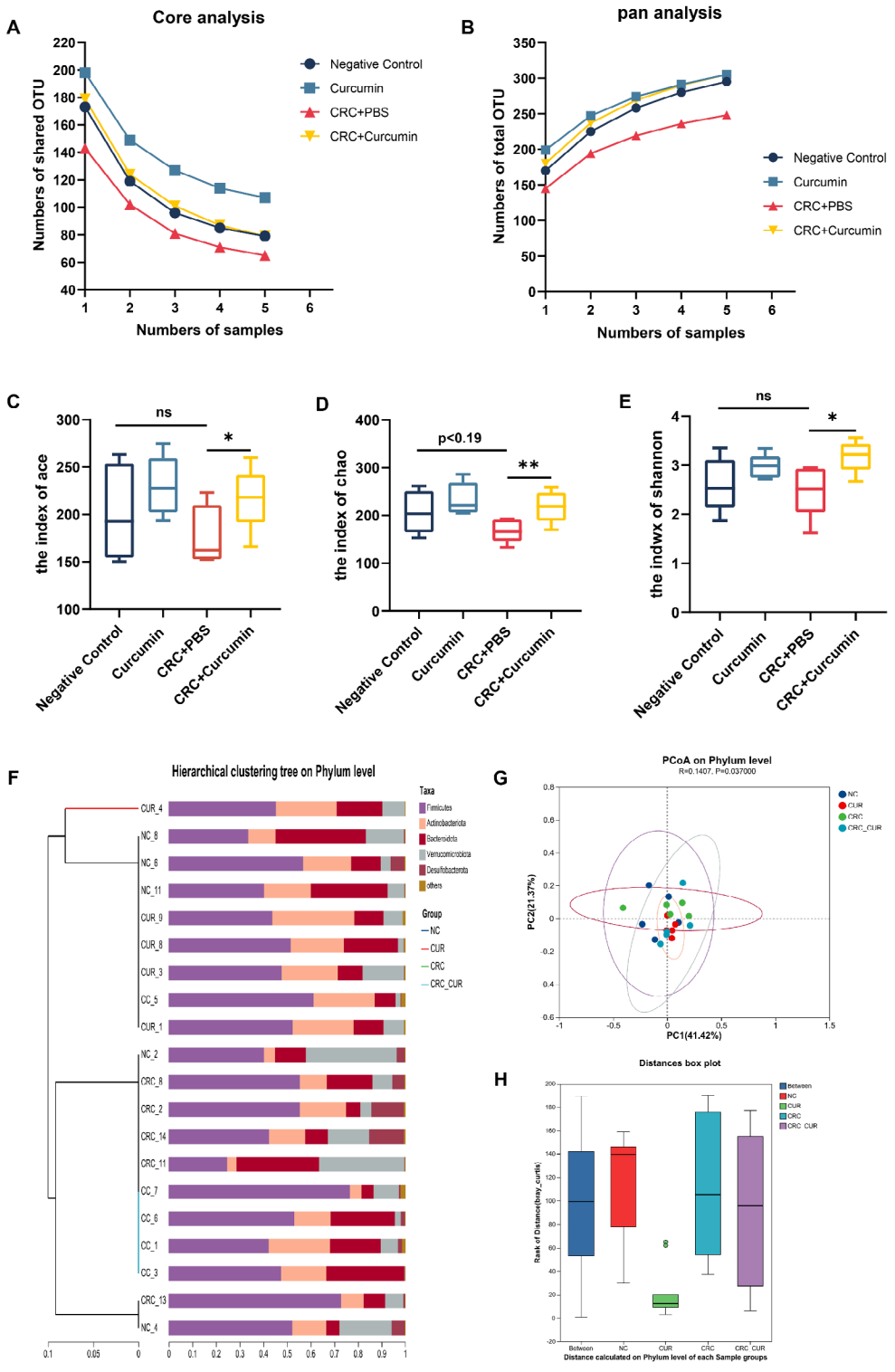

Fig. 2 The impact of curcumin on the diversity of gut microbiota. (**A**) Core analysis of the four groups at the OTU level. (**B**) Pan analysis of the four groups at the OTU level. (**C**), (**D**), (**E**) Alpha diversity of the gut microbiome in the four groups according to the ace, chao and shannon indices. (**F**) Hierarchical clustering analysis (HCA) of the metabolites in the four groups based on their z-normalized abundances at the phylum level. (**G**) Principal coordinate analysis (PCoA, beta diversity) of the gut microbiome in the four groups at the phylum level. (**H**) ANOSIM/Adonis similarity analysis of the gut microbiome in the four groups. $^{*}P < 0.05$, $^{**}P < 0.01$. $n = 5$

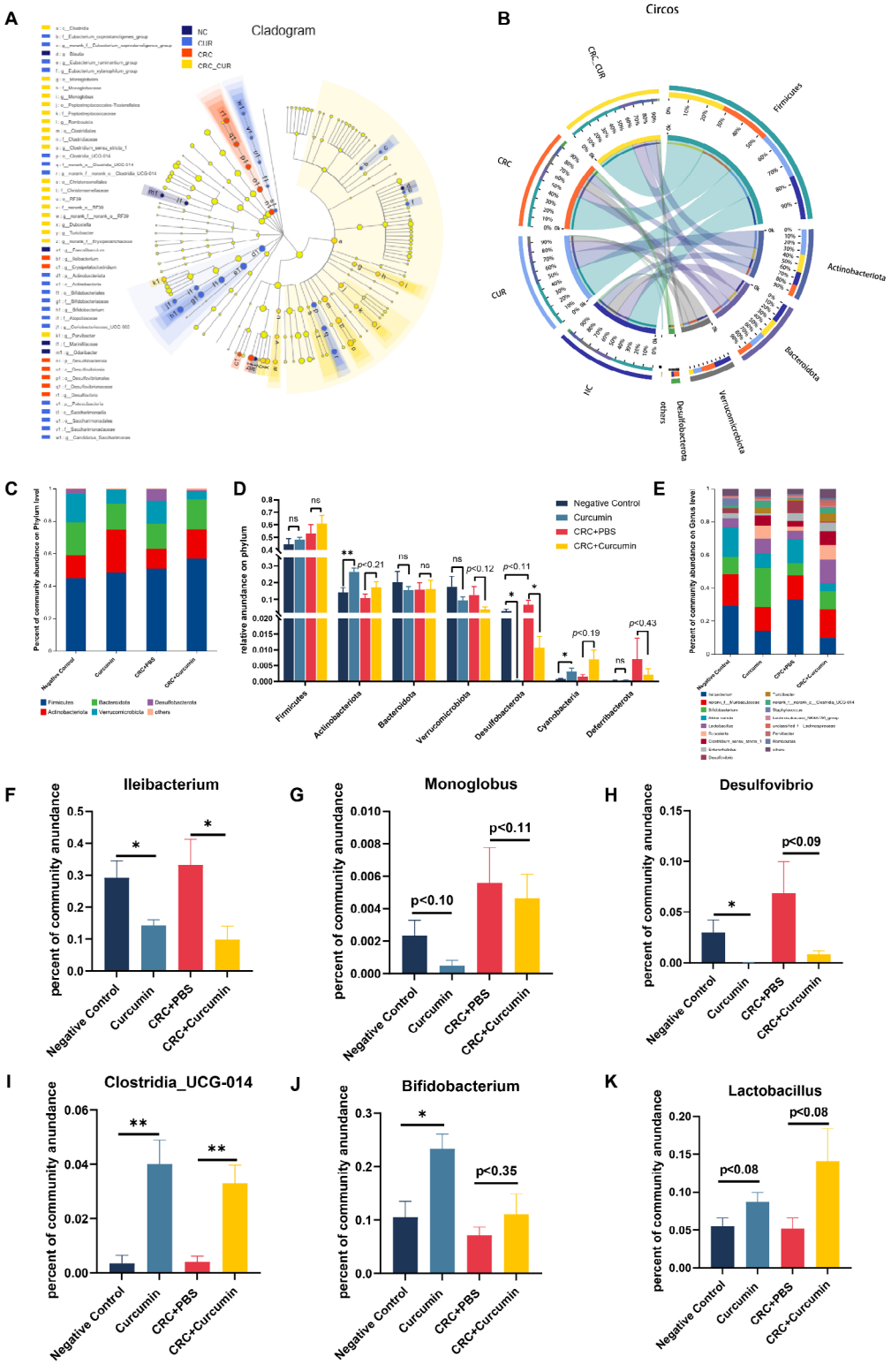

Fig. 3 Effects of curcumin on the gut microbiota composition and taxa abundance. (**A**) LEfSe multi-level differential analysis of taxa (from phylum level to genus level). (**B**) Circos plot of sample-taxa relationships (phylum level). (**C**) Composition of the gut microbiota at the phylum level. (**D**) Relative abundance of taxa in each group at the phylum level. (**E**) Composition of the gut microbiota at the genus level. (**F**) Relative abundance of *Ileibacterium* in each group. (**G**) Relative abundance of *Monoglobus* in each group. (**H**) Relative abundance of *Desulfovibrio* in each group. (**I**) Relative abundance of *Clostridia_UCG-014* in each group. (**J**) Relative abundance of *Bifidobacterium* in each group. (**K**) Relative abundance of *Lactobacillus* in each group. $^{*}P < 0.05$, $^{**}P < 0.01$. $n = 5$

to the NC and CRC model groups, curcumin treatment markedly increased the abundance of *Clostridia_UCG-014* in mouse stool ($p<0.01$, Fig. 3I). The abundances of *Bifidobacterium* ($p<0.05$ and $p<0.35$, Fig. 3J) and *Lactobacillus* ($p<0.08$, Fig. 3K) also showed varying degrees of increase. These results highlight curcumin's ability to reduce the colonization of harmful bacteria in the gut while simultaneously restoring and increasing the abundance of beneficial bacteria.

Curcumin regulates gut metabolites in AOM/DSS-induced CRC mice

Intestinal metabolites are closely associated with the onset and progression of CRC. To investigate this possibility, we randomly selected fecal samples from five mice in each group and conducted a detailed analysis of metabolite variations using LC–MS. Principal component analysis (PCA) and partial least squares discriminant analysis (PLS-DA) were used to distinguish the gut metabolite profiles of the NC, curcumin, CRC, and curcumin-CRC groups (Fig. 4A-B). In the comparison of differential gut metabolites, we identified 249 distinct metabolites between the curcumin group and the NC group, 151 between the CRC model group and the NC group, and 265 between the curcumin-CRC group and the CRC group (Fig. 4C). Further Venn analysis unveiled 13 common differentially abundant metabolites among the three groups (Fig. 4C). Finally, by querying the HMDB 4.0 database, we analyzed the classification information for these 13 metabolites. As depicted in Fig. 4D; Table 1, the HMDB compound classifications were as follows: alkanes and ketones (33.33%), organic acids and derivatives (25.00%), nucleosides and nucleotides and their analogs (16.67%), organoheterocyclic compounds (16.67%), and lipids and lipid-like molecules (8.33%).

We conducted a detailed analysis of the relative abundance of the 13 shared differentially abundant metabolites. As depicted in Fig. 5A-B, in the DSS/AOM-induced CRC model group, ethosuximide, xanthosine, and 17-beta-estradiol 3-sulfate-17-(beta-D-glucuronide) exhibited considerable increases compared to those in the NC group, while curcumin treatment profoundly mitigated the elevation of these metabolites. Furthermore, compared with those in the NC group, the model group exhibited notable reductions in glutamylleucine, gamma-glutamylleucine, liquiritin, ubenimex, 5'-deoxy-5'-fluorouridine, 7,8-dihydropteroic acid, neobyakangelicol, libenzapril, xenognosin A, and 7,4'-dihydroxy-8-methylflavan. It is important to note that curcumin treatment upregulated the above downregulated metabolites. Interestingly, based on the metabolomic data, enrichment bubble plots of Kyoto Encyclopedia of Genes and Genome (KEGG) pathways (Fig. 5C; Table 2) revealed that these 13 differentially abundant metabolites were predominantly enriched in seven pathways, encompassing folate biosynthesis, drug metabolism-other enzymes, biosynthesis of amino acids and alkaloids derived from purines, purine metabolism, caffeine metabolism, ABC transporters, and biosynthesis of cofactors ($P<0.05$), with folate biosynthesis exhibiting the greatest difference ($P=0.0485$). These findings indicate a substantial alteration in the relative abundance of intestinal metabolites in AOM/DSS-induced CRC mice, and curcumin effectively counteracts these changes in the relative abundance of intestinal metabolites. Curcumin may alleviate the development of CRC in mice by modulating the above seven pathways.

Discussion

Numerous studies have highlighted the association of gut microbiota and its metabolites in the development and progression of CRC [5, 9, 25]. In addition, although curcumin shows promise for CRC prevention and treatment, its mechanisms remain unknown. In this study, we established an AOM/DSS-induced CRC model to investigate if curcumin inhibits CRC tumorigenesis by modulating gut microbiota and its metabolites. Compared to the NC group, significant weight loss, reduced colonic length, extensive tumor formation, and pathological changes were observed in the mice of model group, indicating that the successful CRC mouse model was established in this study. Although oral gavage of curcumin did not alleviate weight loss in CRC mice, it did ameliorate AOM/DSS-induced colon shortening and tumor formation. Additionally, it restored the pathological structural morphology of the colon. These findings suggested that curcumin could attenuate AOM/DSS-induced CRC.

We initially investigated the overall effect of curcumin on gut microbiota. 16 S rRNA sequencing analysis revealed that curcumin effectively combats the intestinal dysbiosis induced by CRC. It should be noted that curcumin significantly diminished the relative abundance of harmful bacteria in CRC, such as *Ileibacterium*, *Monoglobus* and *Desulfovibrio*. Simultaneously, it reinstated and elevated the relative abundance of probiotics, including *Clostridia_UCG-014*, *Bifidobacterium* and *Lactobacillus*. The altered abundance of *Ileibaterium* is consistent with previous studies suggesting that it is a harmful bacterium associated with CRC and colitis [26, 27]. *Desulfovibrio* was highly enriched in the AOM/DSS-induced CRC mouse model, representing a typical sulfate-reducing bacterium capable of generating hydrogen sulfide (H_2S) [28]. Elevated concentrations of H_2S in the intestines can compromise mucosal integrity and potentiate genotoxicity [29]. The enrichment of *Monoglobus* contributes to heightened blood ammonia levels, disrupting the barrier function of intestinal epithelial cells, abnormally increasing intestinal permeability, and

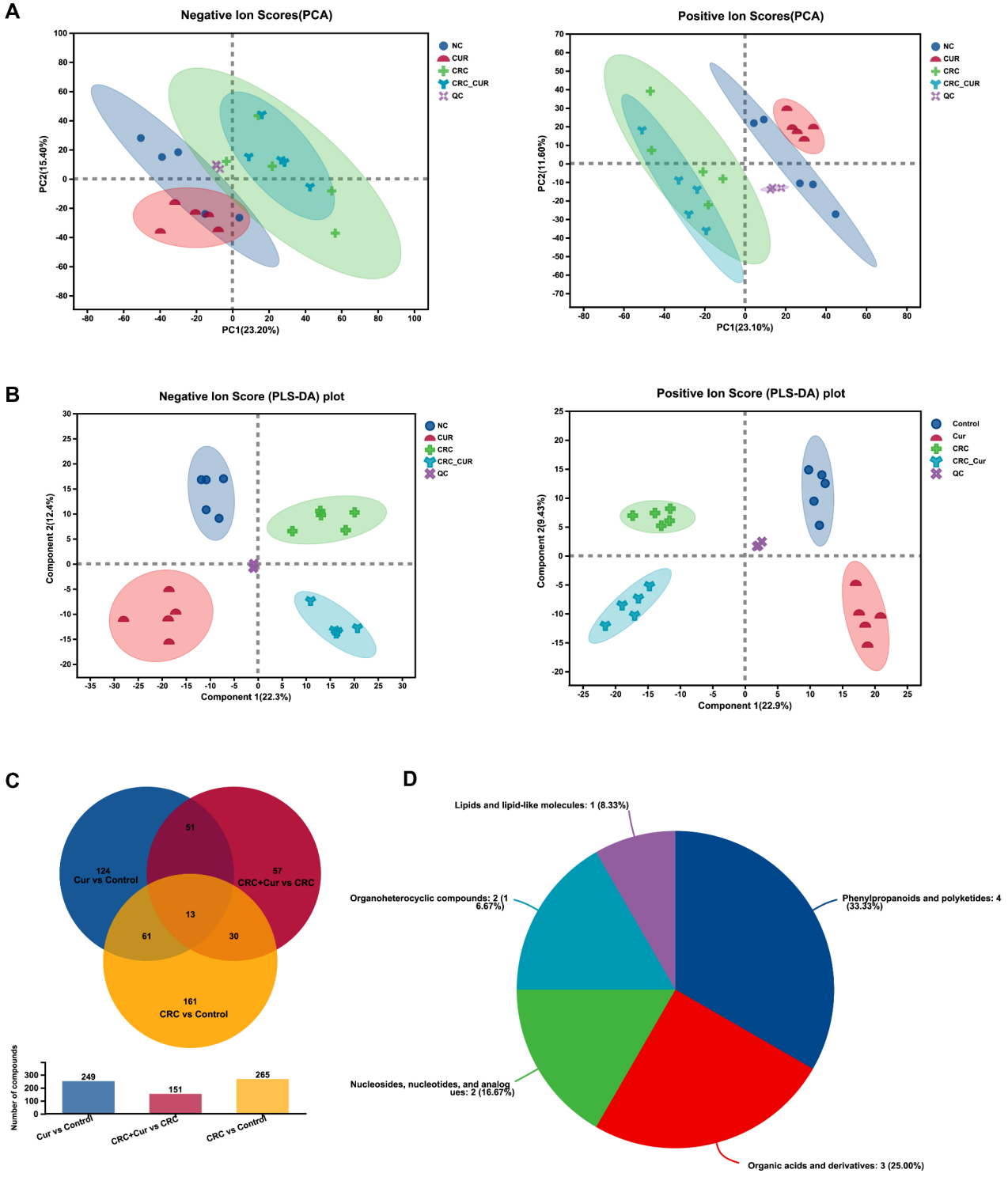

Fig. 4 Curcumin regulates gut microbiota–related metabolites in the stool. (**A**) Negative and positive principal component analysis (unit variance conversion [UV]). (**B**) Negative and positive PLS-DA discriminant analysis (Pareto conversion [Par]). (**C**) Venn diagram of the metabolic sets for the NC group-curcumin group, NC group-CRC group, and CRC group-curcumin-treated CRC group. (**D**) HMDB compound classification pie chart of common differentially abundant metabolites of three metabolic sets for the NC group-curcumin group, NC group-CRC group, and CRC group-curcumin-treated CRC group. $n = 5$

Table 1 Small molecule metabolites set disturbed by curcumin after AOM/DSS-induced CRC in mice

Metab ID	Metabolite	Superclass
1154	Liquiritin	Phenylpropanoids and polyketides
8967	Neobyakangelicol	Phenylpropanoids and polyketides
9048	Xenognosin A	Phenylpropanoids and polyketides
9299	7,4′-Dihydroxy-8-methylflavan	Phenylpropanoids and polyketides
739	Libenzapril	Organic acids and derivatives
941	Glutamylleucine	Organic acids and derivatives
3803	Gamma-glutamylleucine	Organic acids and derivatives
543	5′-Deoxy-5′-fluorouridine	Nucleosides, nucleotides, and analogues
5639	Xanthosine	Nucleosides, nucleotides, and analogues
3705	7,8-Dihydropteroic acid	Organoheterocyclic compounds
4018	Ethosuximide	Organoheterocyclic compounds
5465	17-beta-estradiol 3-sulfate-17-(beta-D-glucuronide)	Lipids and lipid-like molecules
3341	Ubenimex	

triggering systemic inflammation [30]. *Bifidobacterium*, a well-known probiotic, along with *Clostridia-UCG-014*, exerts antitumor effects by regulating intestinal function and enhancing immunity [31, 32]. *Lactobacillus* is also a well-known beneficial bacterium that maintains normal intestinal function and has been shown to prevent CRC [33, 34]. Thus, curcumin facilitated the dominance of probiotics in the gut, playing a pivotal role in stabilizing intestinal pH, safeguarding intestinal permeability, mitigating intestinal inflammation, and suppressing the invasion of pathogenic microorganisms [35]. It is important to note that we chose 16 S rRNA sequencing due to its cost-effectiveness and adequate resolution for assessing microbial differences. We recognized that whole genome sequencing (WGS) provides more detailed information with greater sensitivity and specificity [36]. Future investigations could focus on detecting remarkable changes in specific bacterial abundances in CRC patients, serving as potential biomarkers for disease screening, prognosis, and treatment response prediction. Modulating the gut microbiota with curcumin could be a feasible therapeutic strategy to augment the efficacy of treatment and reduce adverse reactions.

Microbes in the intestines produce a myriad of metabolites that can exert either harmful or beneficial effects on the human body. Numerous studies have highlighted a close association between gut metabolites and the onset and progression of CRC [37, 38]. Hence, we employed LC-MS analysis to investigate differentially abundant metabolites. Among the 13 differentially abundant metabolites, curcumin notably decreased the relative abundance of metabolites elevated in CRC, such as ethosuximide, xanthosine, and 17-beta-estradiol 3-sulfate-17-(beta-D-glucuronide). Xanthosine (a nucleoside) is derived from xanthine and ribose and is linked to the caffeine metabolism pathway in plants [39]. Studies have demonstrated that lowering the relative abundance of xanthosine can alleviate inflammation and CRC symptoms in mice [40]. Furthermore, curcumin restored and augmented the diminished metabolites in CRC, including glutamylleucine, gamma-glutamylleucine, liquiritin, ubenimex, 5′-deoxy-5′-fluorouridine, neobyakangelicol, libenzapril, xenognosin A, 7,4′-dihydroxy-8-methylflavan, and 7,8-dihydropteroic acid. Research has validated the antitumor effects of 5′-deoxy-5′-fluorouridine on human CRC cells [41]. Ubenimex, an immunosuppressant, forms a conjugate with 5′-fluorouridine, thereby enhancing its anticancer functions [42, 43]. This finding is consistent with our observation of a negative correlation between 5′-deoxy-5′-fluorouridine, ubenimex, and CRC. Neobyakangelicol has been shown to possess notable anticancer properties [44]. As dipeptides, glutamylleucine and gamma-glutamylleucine represent incomplete degradation products of macromolecular proteins. They play a role in cell signal transduction and likely function as cell signaling factors relevant to CRC [45]. 7,8-Dihydropteroic acid plays a crucial role in the synthesis and conversion of purine nucleotides and pyrimidine nucleosides [46]. Studies have indicated that dihydrofolate reductase is inhibited in human CRC HCT-116 cell lines, resulting in impaired folate-mediated biosynthesis [47]. Increasing the content of 7,8-dihydropteroic acid by curcumin can promote the recovery of this biological process. Previous reports have primarily associated liquiritin with anti-inflammatory effects [48, 49]. An increase in the relative abundance of liquiritin might impede CRC progression through its anti-inflammatory properties. The roles of several other differentially abundant metabolites remain ambiguous. Therefore, it can be concluded that curcumin decelerates CRC progression by modulating gut metabolites.

Due to its ability to promote beneficial effects on the gut microbiota and metabolites in the CRC model, we further elucidated the curcumin-inhibited signaling pathways in CRC through KEGG analysis. Differentially abundant metabolites were predominantly enriched in seven pathways, encompassing folate biosynthesis, drug metabolism-other enzymes, biosynthesis of amino acids and alkaloids derived from purine metabolism, purine metabolism, caffeine metabolism, ABC transporters, and

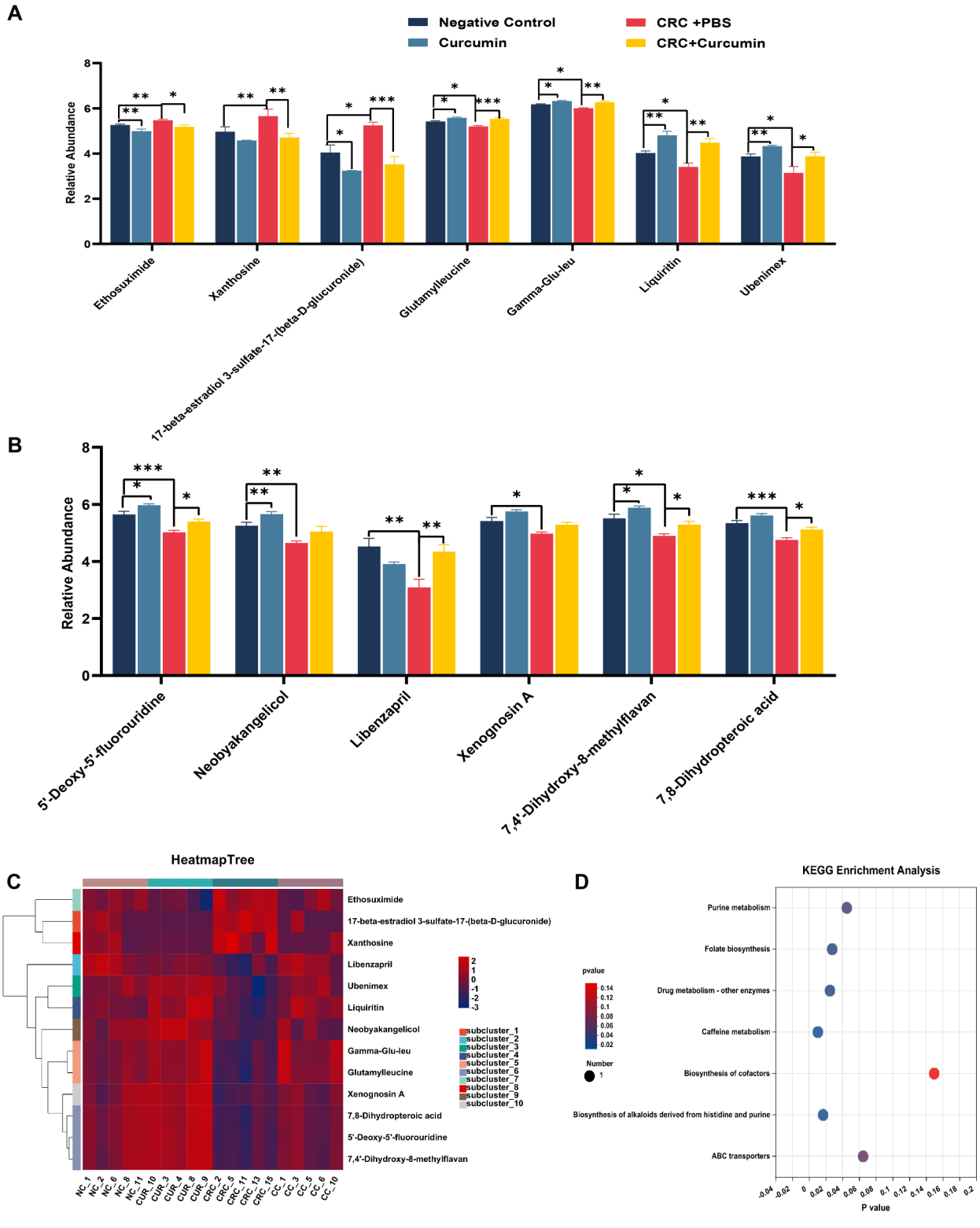

Fig. 5 Relative abundance and enrichment pathways of the 13 differentially abundant metabolites. (**A**) (**B**) Statistical plots of the relative abundance of different metabolites shared by the three metabolites in the NC group-curcumin group, NC group-CRC group, and CRC group-curcumin-treated CRC group. (**C**) Cluster heatmap of shared differentially abundant metabolites. (**D**) KEGG pathway enrichment analysis of shared differentially abundant metabolites. *$P < 0.05$, **$P < 0.01$. $n = 5$

Table 2 Statistical summary of metabolic pathway information for differentially expressed metabolites

Pathway ID	Pathway Description	Total number of metabolites	*P* value
map00790	Folate biosynthesis	58	0.0485
map00983	Drug metabolism - other enzymes	52	0.0581
map01065	Biosynthesis of alkaloids derived from histidine and purine	35	0.0588
map00230	Purine metabolism	95	0.0632
map00232	Caffeine metabolism	22	0.0741
map02010	ABC transporters	137	0.0755
map01240	Biosynthesis of cofactors	327	0.1497

biosynthesis of cofactors. This indicates that curcumin may impede CRC progression through these pathways.

Conclusions

In summary, this study delved into the suppressive impact of curcumin on the histopathology of CRC and revealed its beneficial effects on the diversity, composition, and metabolites of the gut microbiota. The gut microecological balance in AOM/DSS-induced CRC mice were disrupted, accompanied by metabolite dysbiosis. Curcumin restored the equilibrium of the microbiota and regulated metabolites, thereby attenuating the occurrence and progression of CRC. This research innovatively sheds light on the microbiome and metabolomics to explore the intestinal microecological effects of curcumin on CRC. Consequently, we have identified a potential new mechanism for its role in mitigating CRC development.

Supplementary Information

The online version contains supplementary material available at https://doi.org/10.1186/s12885-024-12898-z.

Supplementary Material 1

Acknowledgements

I would like to thank Jie Chen and Zhimin Tang for their valuable guidance on the methods used in this study. I also appreciate Mengchao Liu for his assistance with the animal procedures.

Author contributions

Wenxin Deng and Xiaojian Xiong performed the experiments and wrote the manuscript. Mingyang Lu analyzed the data. Shibo Huang and Yujie Wang analyzed and discussed results. Yunfei Luo helped with the in vivo experiments. Ying Ying conceived the study design, supervised the scientific work and revised the manuscript. All the authors reviewed the draft and approved the final manuscript before submission.

Funding

The work was supported by the National Natural Science Foundation of China (No. 32260168), the Natural Science Foundation of Jiangxi Province (20232BAB206163 and 20212BAB206039).

Data availability

The datasets used during the study are available from the corresponding author upon reasonable request.

Declarations

Ethics approval and consent to participate

All animal experiments were conducted in compliance with the ethical standards set by the Experimental Animal Ethics Committee of Nanchang University, following the guidelines for standard experimental animals.

Consent for publication

Not applicable.

Competing interests

The authors declare no competing interests.

Author details

[1]Jiangxi Provincial Key Laboratory of Prevention and Treatment of Infectious Diseases, Jiangxi Medical Center for Critical Public Health Events, The First Affiliated Hospital, Jiangxi Medical College, Nanchang University, Nanchang 330052, Jiangxi, P.R. China
[2]Department of Pathophysiology, School of Basic Medical Sciences, Jiangxi Medical College, Nanchang University, Nanchang 330006, Jiangxi, P.R. China
[3]Queen Mary School, Nanchang University, Nanchang 330006, Jiangxi, P.R. China
[4]The Clinical Trial Research Center, The First Affiliated Hospital, Jiangxi Medical College, Nanchang University, Nanchang 330052, Jiangxi, P.R. China
[5]Department of Metabolism and Endocrinology, The Second Affiliated Hospital, Jiangxi Medical College, Nanchang University, Nanchang 330006, Jiangxi, P.R. China
[6]Jiangxi Provincial Key Laboratory of Respiratory Diseases, Jiangxi Institute of Respiratory Diseases, The Department of Respiratory and Critical Care Medicine, The First Affiliated Hospital, Jiangxi Medical College, Nanchang University, Nanchang 330006, China

Received: 29 March 2024 / Accepted: 3 September 2024
Published online: 12 September 2024

References

1. Siegel RL, Wagle NS, Cercek A, et al. Colorectal cancer statistics, 2023 [J]. CA Cancer J Clin. 2023;73(3):233–54.
2. Dekker E, Tanis PJ, Vleugels JLA, et al. Colorectal cancer [J]. Lancet. 2019;394(10207):1467–80.
3. Fan A, Wang B, Wang X, et al. Immunotherapy in colorectal cancer: current achievements and future perspective [J]. Int J Biol Sci. 2021;17(14):3837–49.
4. Van Der Jeught K, Xu HC, Li YJ, et al. Drug resistance and new therapies in colorectal cancer [J]. World J Gastroenterol. 2018;24(34):3834–48.
5. Song M, Chan AT, Sun J. Influence of the gut microbiome, diet, and environment on risk of colorectal cancer [J]. Gastroenterology. 2020;158(2):322–40.
6. Wong SH, Zhao L, Zhang X, et al. Gavage of fecal samples from patients with colorectal cancer promotes intestinal carcinogenesis in germ-free and conventional mice [J]. Gastroenterology. 2017;153(6):1621–e336.
7. Wong SH. Gut microbiota in colorectal cancer: mechanisms of action and clinical applications [J]. Nat Reviews Gastroenterol Hepatol. 2019;16(11):690–704.
8. Hou H, Chen D, Zhang K, et al. Gut microbiota-derived short-chain fatty acids and colorectal cancer: ready for clinical translation? [J]. Cancer Lett. 2022;526:225–35.
9. Ternes D, Tsenkova M, Pozdeev VI, et al. The gut microbial metabolite formate exacerbates colorectal cancer progression [J]. Nat Metabolism. 2022;4(4):458–75.
10. Pricci M, Girardi B, Giorgio F et al. Curcumin and colorectal cancer: from basic to clinical evidences [J]. Int J Mol Sci. 2020;21(7).
11. Chen CY, Kao CL, Liu CM. The cancer prevention, anti-inflammatory and anti-oxidation of bioactive phytochemicals targeting the TLR4 signaling pathway [J]. Int J Mol Sci. 2018;19(9).
12. Eke-Okoro UJ, Raffa RB, Pergolizzi JV JR, et al. Curcumin in turmeric: basic and clinical evidence for a potential role in analgesia [J]. J Clin Pharm Ther. 2018;43(4):460–6.
13. Naeini MB, Momtazi AA, Jaafari MR, et al. Antitumor effects of curcumin: a lipid perspective [J]. J Cell Physiol. 2019;234(9):14743–58.

14. Li G, Fang S, Shao X et al. Curcumin reverses NNMT-induced 5-fluorouracil resistance via increasing ROS and cell cycle arrest in colorectal cancer cells [J]. Biomolecules. 2021;11(9).
15. Brockmueller A, Ruiz de Porras V, Shakibaei M. Curcumin and its anti-colorectal cancer potential: from mechanisms of action to autophagy [J]. Phytother Res. 2024;38(7):3525–51.
16. Li J, Chai R, Chen Y et al. Curcumin targeting non-coding RNAs in colorectal cancer: therapeutic and biomarker implications [J]. Biomolecules. 2022;12(10).
17. Liu C, Rokavec M, Huang Z, et al. Curcumin activates a ROS/KEAP1/NRF2/miR-34a/b/c cascade to suppress colorectal cancer metastasis [J]. Cell Death Differ. 2023;30(7):1771–85.
18. Hashemi M, Abbaszadeh S, Rashidi M, et al. STAT3 as a newly emerging target in colorectal cancer therapy: tumorigenesis, therapy response, and pharmacological/nanoplatform strategies [J]. Environ Res. 2023;233:116458.
19. Howells LM, Iwuji COO, Irving GRB, et al. Curcumin combined with FOLFOX chemotherapy is safe and tolerable in patients with metastatic colorectal cancer in a randomized phase IIa trial [J]. J Nutr. 2019;149(7):1133–9.
20. Scazzocchio B, Minghetti L, D'Archivio M. Interaction between gut microbiota and curcumin: a new key of understanding for the health effects of curcumin [J]. Nutrients. 2020;12(9).
21. Feng W, Wang H, Zhang P, et al. Modulation of gut microbiota contributes to curcumin-mediated attenuation of hepatic steatosis in rats [J]. Biochim Biophys Acta Gen Subj. 2017;1861(7):1801–12.
22. Zhong, Y-B, Kang Z-P, Wang M-X et al. Curcumin ameliorated dextran sulfate sodium-induced colitis via regulating the homeostasis of DCs and Treg and improving the composition of the gut microbiota [J]. J Funct Foods. 2021;86.
23. Luca SV, Macovei I, Bujor A, et al. Bioactivity of dietary polyphenols: the role of metabolites [J]. Crit Rev Food Sci Nutr. 2020;60(4):626–59.
24. Kasprzak-Drozd K, Oniszczuk T, Gancarz M et al. Curcumin and weight loss: does it work? [J]. Int J Mol Sci. 2022;23(2).
25. Wong CC, Yu J. Gut microbiota in colorectal cancer development and therapy [J]. Nat Rev Clin Oncol. 2023;20(7):429–52.
26. Fu T, Huan T, Rahman G et al. Paired microbiome and metabolome analyses associate bile acid changes with colorectal cancer progression [J]. Cell Rep. 2023;42(8).
27. Lin H, Ma X, Yang X et al. Natural shikonin and acetyl-shikonin improve intestinal microbial and protein composition to alleviate colitis-associated colorectal cancer [J]. Int Immunopharmacol. 2022;111.
28. Zhao H, He M, Zhang M, et al. Colorectal cancer, gut microbiota and traditional Chinese medicine: a systematic review [J]. Am J Chin Med. 2021;49(4):805–28.
29. Braccia DJ, Jiang X, Pop M, et al. The capacity to produce hydrogen sulfide (H(2)S) via cysteine degradation is ubiquitous in the human gut microbiome [J]. Front Microbiol. 2021;12:705583.
30. Sakurai K, Toshimitsu T. Okada E, et al. Effects of lactiplantibacillus plantarum OLL2712 on memory function in older adults with declining memory: a randomized placebo-controlled trial [J]. Nutrients. 2022;14(20).
31. Liu L, Shah K. The potential of the gut microbiome to reshape the cancer therapy paradigm: a review [J]. JAMA Oncol. 2022;8(7):1059–67.
32. Zha H, Si G, Wang C et al. Multiple intestinal bacteria associated with the better protective effect of bifidobacterium pseudocatenulatum LI09 against rat liver injury [J]. Biomed Res Int. 2022;2022:8647483.
33. Sugimura N, Li Q, Chu ESH, et al. Lactobacillus gallinarummodulates the gut microbiota and produces anti-cancer metabolites to protect against colorectal tumourigenesis [J]. Gut. 2022;71(10):2011–21.
34. Wang Z, Dan W, Zhang N et al. Colorectal cancer and gut microbiota studies in China [J]. Gut Microbes. 2023;15(1).
35. Yu J, Feng Q, Wong SH, et al. Metagenomic analysis of faecal microbiome as a tool towards targeted non-invasive biomarkers for colorectal cancer [J]. Gut. 2017;66(1):70–8.
36. Church DL, Cerutti L, Gürtler A et al. Performance and application of 16S rRNA gene cycle sequencing for routine identification of bacteria in the clinical microbiology laboratory [J]. Clin Microbiol Rev. 2020;33(4).
37. Dalal N, Jalandra R, Bayal N, et al. Gut microbiota-derived metabolites in CRC progression and causation [J]. J Cancer Res Clin Oncol. 2021;147(11):3141–55.
38. Chen F, Dai X, Zhou CC, et al. Integrated analysis of the faecal metagenome and serum metabolome reveals the role of gut microbiome-associated metabolites in the detection of colorectal cancer and adenoma [J]. Gut. 2022;71(7):1315–25.
39. Ashihara H, Monteiro AM, Gillies FM, et al. Biosynthesis of caffeine in leaves of coffee [J]. Plant Physiol. 1996;111(3):747–53.
40. Ma F, Sun M, Song Y et al. Lactiplantibacillus plantarum-12 alleviates inflammation and colon cancer symptoms in AOM/DSS-treated mice through modulating the intestinal microbiome and metabolome [J]. Nutrients. 2022;14(9).
41. Zhang J, Mizoi T, Harada N, et al. Thymidine phosphorylase expressed in macrophages enhances antitumor effect of 5'-deoxy-5-fluorouridine on human colorectal carcinoma cells [J]. Anticancer Res. 2003;23(1A):323–9.
42. Jiang Y, Li X, Hou J, et al. Synthesis and biological characterization of ubenimex-fluorouracil conjugates for anti-cancer therapy [J]. Eur J Med Chem. 2018;143:334–47.
43. Ota K. Review of ubenimex (Bestatin): clinical research [J]. Biomed Pharmacother. 1991;45(2–3):55–60.
44. Okuyama T, Takata M, Nishino H, et al. Studies on the antitumor-promoting activity of naturally occurring substances. II. Inhibition of tumor-promoter-enhanced phospholipid metabolism by umbelliferous materials [J]. Chem Pharm Bull (Tokyo). 1990;38(4):1084–6.
45. Janaky R, Shaw CA, Varga V, et al. Specific glutathione binding sites in pig cerebral cortical synaptic membranes [J]. Neuroscience. 2000;95(2):617–24.
46. Blakley RL. Dismutation of dihydrofolate by dihydrofolate reductase [J]. Biochemistry. 1984;23(11):2377–83.
47. Chen L, Zhang Z, Hoshino A, et al. NADPH production by the oxidative pentose-phosphate pathway supports folate metabolism [J]. Nat Metab. 2019;1:404–15.
48. Yang X, Dang X, Zhang X, et al. Liquiritin reduces lipopolysaccharide-aroused HaCaT cell inflammation damage via regulation of microRNA-31/MyD88 [J]. Int Immunopharmacol. 2021;101(Pt B):108283.
49. Zhai KF, Duan H, Cui CY, et al. Liquiritin from glycyrrhiza uralensis attenuating rheumatoid arthritis via reducing inflammation, suppressing angiogenesis, and inhibiting MAPK signaling pathway [J]. J Agric Food Chem. 2019;67(10):2856–64.

Publisher's note